

Reflection Resonances in a Washboard Potential

Erica Caden

Quantum Mechanics II

Term Project

June 2, 2003

This paper analyses the reflection resonances in a washboard potential. To better understand what is happening in the washboard potential, different linear potential barrier were studied, as well as a hyperbolic-tangent shaped potential. A resonance occurs when the phase shift, $\phi(E)$, undergoes a rapid change of 2π radians. The phase angle shows a Lorentzian line shape and from the equation of the line we can find the energy E_0 and lifetime γ of the quasi-bound state. This is applicable to a differential reflection resonance interferometer.

1 Introduction

When a beam of energy beam is shot at a potential barrier, it is either transmitted or reflected, with some probability. If the transmission probability is very low, the reflection probability is very high[1]. One potential that exhibits 100% reflection probability is the washboard potential, often encountered in biased Josephson Junctions, which themselves are useful in high speed circuits. Our washboard potential is shown in Fig. 1.

Particles that are incident from the left of the potential, with energies between $-10eV$ and $19.4eV$ will be reflected with 100% probability. This means that $R(E) = |r(E)|^2 = 1.0$. $r(E)$ is the reflection probability amplitude, defined by $r(E) = 1e^{2i\phi(E)}$. $r(E)$ goes through resonances where the reflection phase angle $\phi(E)$ goes through rapid shifts. This happens when we scan through a certain, narrow energy range. The resonances can be described by Lorentzian line peaks.

The input and output amplitudes of the energy beam are related through the transfer matrix(notation used in [2]):

$$\begin{bmatrix} A_L \\ B_L \end{bmatrix} = \begin{bmatrix} t_{11}(E) & t_{12}(E) \\ t_{21}(E) & t_{22}(E) \end{bmatrix} \begin{bmatrix} A_R \\ B_R \end{bmatrix}$$

For a reflecting boundary, $t_{21}(E) = t_{11}(E)^*$. The first element of the transmission matrix is given by $t_{11}(E) = a(E) + ib(E)$. The reflection probability amplitude and the phase angle are

$$r(E) = t_{21}(E)/t_{11}(E) \quad (1)$$

$$\phi(E) = \tan^{-1} b(E)/a(E) \quad (2)$$

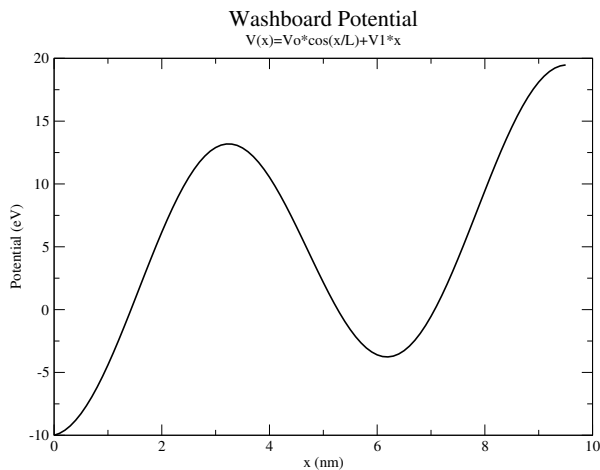


Figure 1:
The Washboard Potential. $V_0 = -10eV$, $L = 1nm$, $V_1 = 1eV$

2 Preparation

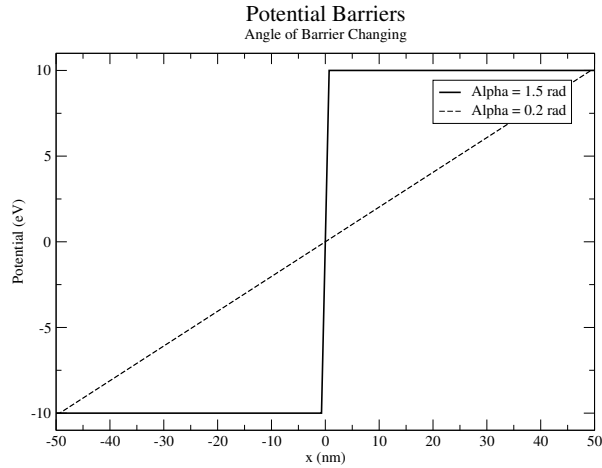


Figure 2: Slanted Potential $V_L = -10eV, V_R = 10eV$. α varies from $0.2rad$ to $1.5 rad$

Before analyzing the washboard potential, we analyzed shifts in the phase angle $\phi(E)$ which occurred from bouncing energy against simpler potentials. The first potential analyzed was a simple slanted potential, where the angle the barrier made with the horizontal asymptotic left and right potentials was changed. Fig. 2 shows the first and last potential barriers against which energy beams were bounced. The beam had an energy of $E = 0eV$ and always hit the potential at $x = 0nm$. The slope of the potential barrier, α , was changed from $\alpha = 0.2 rad$ to $\alpha = 1.5 rad$. The total length of the potential barrier is $100nm$. This is longer than other barriers studied to allow for the range of values of α . The longer the potential barrier is, the more α can be varied. Fig. 3 shows the phase angle, $\phi(E)$, as a function of the slope, α .

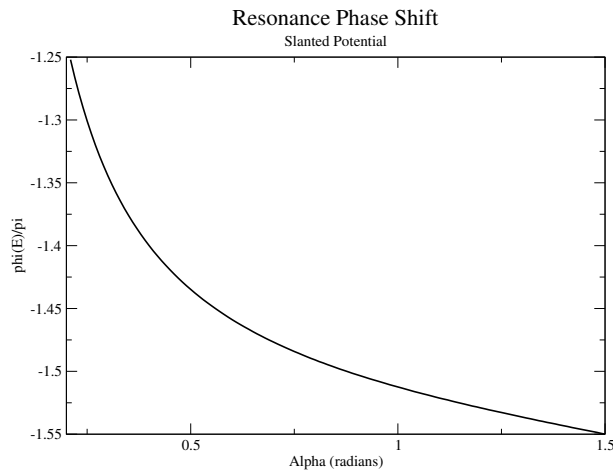


Figure 3: Shift of phase angle $\phi(E)$ of Changing Slope α Potential computed from $t_{11}(E)$ matrix element

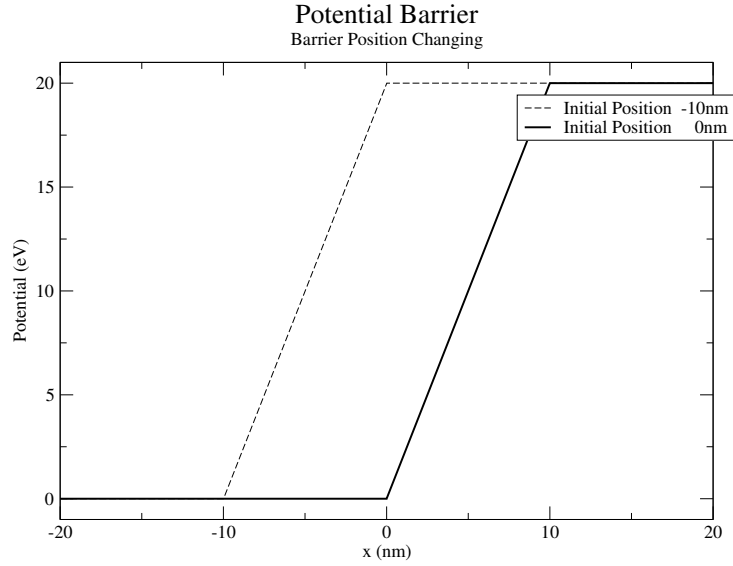


Figure 4: Position of the barrier changing from $x = 0nm$ to $x = -10nm$

In the second step of the preparation, the slope was set a a constant $\alpha = \sqrt{2}/2$ rad. The x position of the start of the barrier was varied. Initially the beginning of the barrier was at $x = 0nm$ and we iterated until the beginning of the barrier was at $x = -10nm$. Fig. 4 shows the initial and final potential barriers against which we bounced energy. Energy beams were sent to hit the barrier at $x = 0nm$ every time so as not to introduce any extra phase shift from one beam traveling further than any other. In order to hit the barrier at a constant spot when the barrier position was changing, we had to scan through different energy levels. The energy of the beam varied from $E = 0ev$ to $E = 19.9eV$. Fig. 5 is a plot of the phase angle, $\phi(E)$, as a function of the energy of the beam.

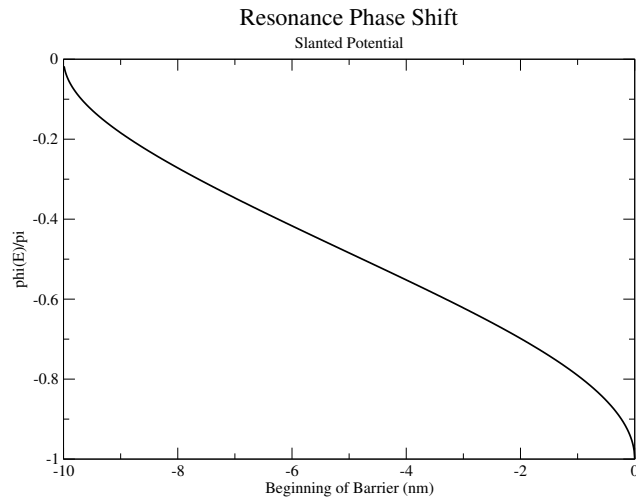


Figure 5: Shift of phase angle $\phi(E)$ of Moving Barrier Potential computed from $t_{11}(E)$ matrix element

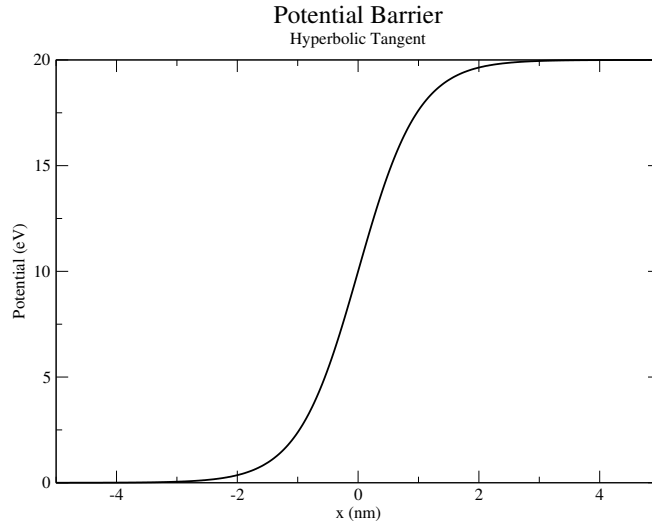


Figure 6: Hyperbolic Tangent Potential Barrier. $V_L = 0eV$ and $V_R = 20eV$. The barrier is $20nm$ wide

For the final step before analyzing the washboard potential, energy beams were bounced off a hyperbolic tangent shaped potential barrier. The barrier was vertically displaced $10eV$ so there would be no sign change in the energies. The width of the barrier was decreased from $20nm$ to $10nm$. In the regions which were removed, the asymptotic potential was not changing. The asymptotic potentials are $V_L = 0eV$ and $V_R = 20eV$. Fig. 6 shows the potential. Energies scanned were from $E = 0eV$ to $E = 19.9eV$. Fig. 7 shows the change in phase angle, $\phi(E)$ as a function of the energy scanned in.

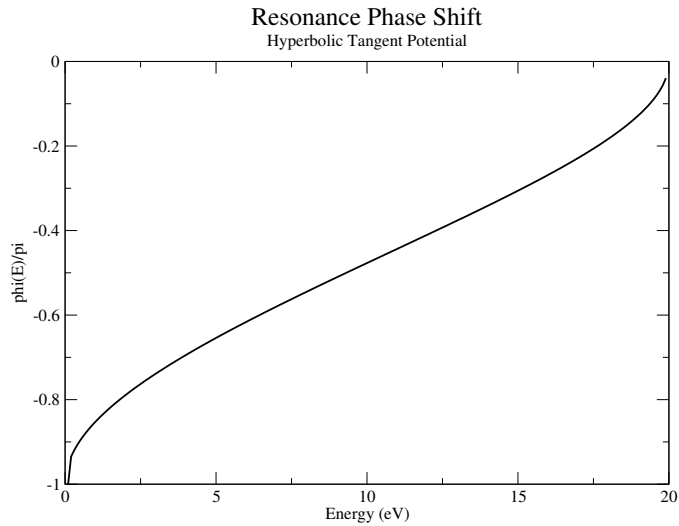


Figure 7: Shift of phase angle $\phi(E)$ computed from $t_{11}(E)$ matrix element

3 Procedure

In looking at Figs. 3, 5, & 7, we observe that all of the shifts in phase angle $\phi(E)$ are smoothly varying and exhibit no sudden changes over the respective independent parameter. Since the shift in phase angle $\phi(E)$ is now reasonably well understood, it had come time to move onto bigger and better things. We bounced energies against a washboard potential, previously shown in Fig. 1. When there is a ‘quasi-stable’ bound state in the potential “well”, there is a resonance in the reflection amplitude, $r(E)$ such that the phase angle $\phi(E)$ undergoes rapid shifts near the energy of the state. A ‘quasi-stable’ bound state means that the lifetime of the state is not infinite and it will decay away. The $t_{11}(E)$ matrix element has the form:

$$t_{11}(E) = e^{-i\theta} [(E - E_0) - i(\hbar\gamma/2)] \quad (1)$$

so $\phi(E)$ has the form

$$\phi(E) = \theta(E) + \tan^{-1} \left(\frac{\hbar\gamma/2}{E - E_0} \right) \quad (2)$$

$\theta(E)$ is slowly varying, so the change in $\phi(E)$, after removing $d\theta(E)/dE$, can be approximated by the Lorentzian line

$$\frac{d\phi(E)}{dE} = \frac{\hbar\gamma/2}{(E - E_0)^2 + (\hbar\gamma/2)^2} \quad (3)$$

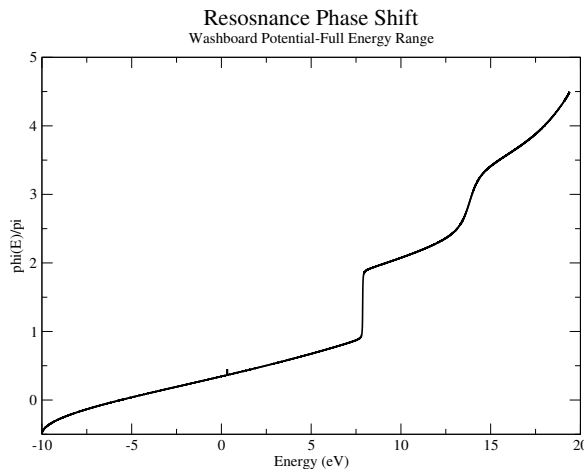


Figure 8: Shift of phase angle $\phi(E)$ for Washboard Potential computed from $t_{11}(E)$ matrix element

As with the previous potentials, the energy of the beam was scanned through the entire energy of the potential. Fig. 8 shows the shift in $\phi(E)$ as a function of energy. We observe that the graph is rather smooth, with a slight “bump” in the graph, occurring just below $E = 8eV$. We then narrowed our energy range to $7.75 \leq E \leq 8.0eV$ and scanned the potential again. Fig. 9 shows the phase angle plotted against the decreased energy range. The sharp change on the graph, which is not present in any of our “test potentials”, shows a resonance and indicates the existence of a quasi-stable bound state. We recognize that

there is a second “bump” in the potential, around $E = 12eV$, but this is due to an excited bound state, and the author of this paper is only concerned with the ‘ground’ bound state.

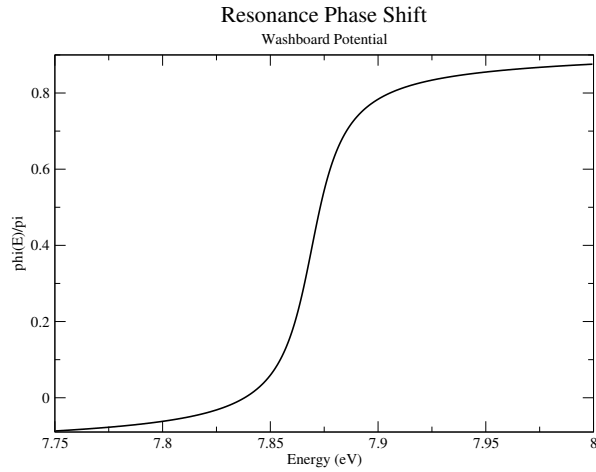


Figure 9: Shift of phase angle $\phi(E)$ for Washboard Potential with cropped Energy range computed from $t_{11}(E)$ matrix element

The real and imaginary parts of $t_{11}(E)$, $a(E)$ and $b(E)$ respectively, are plotted in Fig. 10. Their zero crossing points indicate that yes, there is a resonance in our area of interest. The closer the crossings are to each other, the sharper the resonance is.

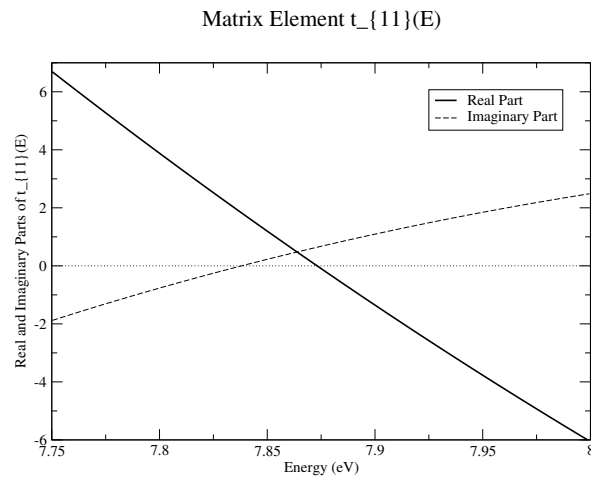


Figure 10: Real and Imaginary parts of the $t_{11}(E)$ Matrix Element with arbitrary scaling.

4 Analysis

We can write $a(E)$ and $b(E)$ in the form

$$a(E) = \alpha(E)(E - E_r) \quad (1)$$

$$b(E) = \beta(E)(E - E_i) \quad (2)$$

where $\alpha(E)$ and $\beta(E)$ are the slopes of the lines and E_r and E_i are their zero crossings, respectively. $\alpha(E)$ and $\beta(E)$ are weakly dependant on E , so near E_r and E_i we can approximate them to be constant, and not be functions of E . Because of this weak dependence,

$$|t_{11}(E)|^2 = a(E)^2 + b(E)^2 \quad (3)$$

$$|t_{11}(E)|^2 = (\alpha^2 + \beta^2)[(E - E + 0)^2 + (\hbar\gamma/2)^2] \quad (4)$$

The inverse of this has the Lorentzian shape, seen in Fig. 11.

$$\frac{1}{|t_{11}(E)|^2} = \frac{\text{const}}{(E - E + 0)^2 + (\hbar\gamma/2)^2}, \quad (5)$$

where

$$\text{const} = \frac{1}{\alpha^2 + \beta^2} \quad (6)$$

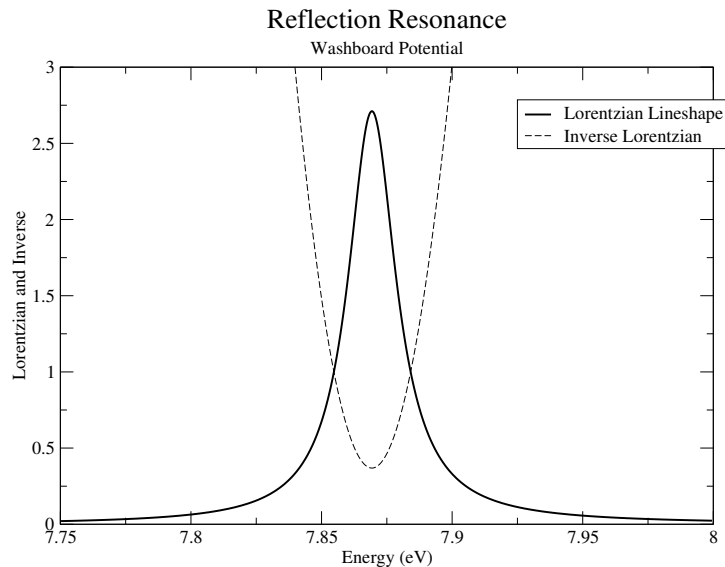


Figure 11: $|t_{11}(E)|^2$ and its inverse in arbitrary units, as functions of Energy

The peak, E_0 , and halfwidth, $\hbar\gamma/2$, of the Lorentzian line are given by

$$E_0 = \frac{\alpha^2 E_r + \beta^2 E_i}{\alpha^2 + \beta^2} \quad (7)$$

$$\hbar\gamma/2 = \frac{|\alpha\beta(E_r - E_i)|}{\alpha^2 + \beta^2} \quad (8)$$

These equations are the weighted averages of the zero-crossings of the real and imaginary parts of $t_{11}(E)$. From Fig. 10 it was calculated that $E_r = 7.873eV$ and $E_i = 7.838eV$. From Fig. 11, we calculated that $E_0 = 7.86925eV$. Using Fig. 10 again, the slopes of $\alpha(E)$ and $\beta(E)$ are $\alpha = -50.91$ and $\beta = 17.46$, in arbitrary units. Using these values, and our calculated values for E_r and E_i , we calculated E_0 to be $7.86932eV$. Their agreement shows that the calculations for $\alpha(E)$ and $\beta(E)$ are reasonable. Using them, we calculated $\hbar\gamma/2 = 0.01074eV$. This leads to $\gamma = 5.1947 \times 10^{12} s^{-1}$, which means that the lifetime of the state is $1.925 \times 10^{-13} s$.

5 Conclusions

For reflecting potentials that possess bound states, the phase shift in the $t_{11}(E)$ matrix element goes through a rapid change of 2π radians when the incident energy passes through a quasi-bound state. This indicates the presence of a reflection resonance. The shape of $1/|t_{11}(E)|$ can be well approximated by a Lorentzian. This Lorentzian can be computed from the real and imaginary parts of $t_{11}(E)$. The energy of the quasi-bound state can be calculated from the Lorentzian, as well as the lifetime of this state. This has applications in differential spectroscopy.

References

- [1] D. Bohm. *Quantum Theory*. Prentice Hall, 1951.
- [2] R. Gilmore. *Elementary Quantum Mechanics in One Dimension*. John Hopkins University Press, 2004.